Molecular Crystals and Liquid Crystals

ISSN: 1542-1406 (Print) 1563-5287 (Online) Journal homepage: http://www.tandfonline.com/loi/gmcl20

Synthesis and Liquid Crystal Properties of Supramolecular Side-Chain Liquid-Crystalline Polymers Containing Poly(acrylic acid) Intermolecular Hydrogen Bonds

P. Kandasamy, R. Keerthiga, S. Vijayalakshmi & T. Kaliyappan

To cite this article: P. Kandasamy, R. Keerthiga, S. Vijayalakshmi & T. Kaliyappan (2015) Synthesis and Liquid Crystal Properties of Supramolecular Side-Chain Liquid-Crystalline Polymers Containing Poly(acrylic acid) Intermolecular Hydrogen Bonds, Molecular Crystals and Liquid Crystals, 606:1, 1-11, DOI: 10.1080/15421406.2014.889531

To link to this article: http://dx.doi.org/10.1080/15421406.2014.889531

Mol. Cryst. Liq. Cryst., Vol. 606: pp. 1–11, 2015

ISSN: 1542-1406 print/1563-5287 online
DOI: 10.1080/15421406.2014.889531

Synthesis and Liquid Crystal Properties of Supramolecular Side-Chain Liquid-Crystalline Polymers Containing Poly(acrylic acid) Intermolecular Hydrogen Bonds

P. KANDASAMY, R. KEERTHIGA, S. VIJAYALAKSHMI, AND T. KALIYAPPAN*

Department of Chemistry, Pondicherry Engineering College, Puducherry, India

Novel supramolecular side-chain liquid-crystalline polymers were prepared from poly(acrylic acid) (PAA) and pyridyl Schiff base derivatives through intermolecular hydrogen-bonding interaction between PAA and nitrogen of pyridyl Schiff base derivatives. PAA used as H-bond donor. Pyridyl Schiff base derivatives used as H-bond acceptors. The existence of H-bonding was confirmed by FT-IR spectroscopy. Polymer complexes exhibited stable thermotropic mesophase. Differential scanning calorimetry, polarized optical microscopy, and X-ray diffraction measurements were used to investigate LC behavior. The complexes exhibited smectic C phase broken-fan shaped texture. On increasing spacer length of substituent, the clearing temperature range of the mesophase increased.

Keywords Liquid crystal; mesogen; self-assembly; smectic; thermal properties

1. Introduction

Side-chain liquid-crystalline polymers (SCLCPs) bearing noncovalent interaction has been found to be interesting topics in material science and optical technologies, due to their special application in electro-optical display, information storage, optical processing, and so on [1–7]. The use of specific intermolecular interactions plays major roles in the supramolecular assembly of liquid crystals. In nature, functional biomolecules, such as nucleic acids, sugar, and protein have hydrogen donor and acceptor moieties, which serve for self-assembly and molecular recognition. The use of self-assembly through specific interactions, such as hydrogen bonding, ionic-dipolar and charge transfer interactions has been recognized as a new strategy for constructing SCLCPs [8,9].

For synthetic liquid crystals, the hydrogen bonding interaction is one of the most prominent and widely used as noncovalent interaction in the design and construction of supramolecular functional materials. A great variety of hydrogen bonds have been used to build the supramolecular mesogenic structures. The hydrogen bonding interaction should

*Address correspondence to T. Kaliyappan, Department of Chemistry, Pondicherry Engineering College, Puducherry 605014, India. E-mail: tkaliyappan2001@pec.edu

Color versions of one or more of the figures in the article can be found online at www.tandfonline.com/gmcl.

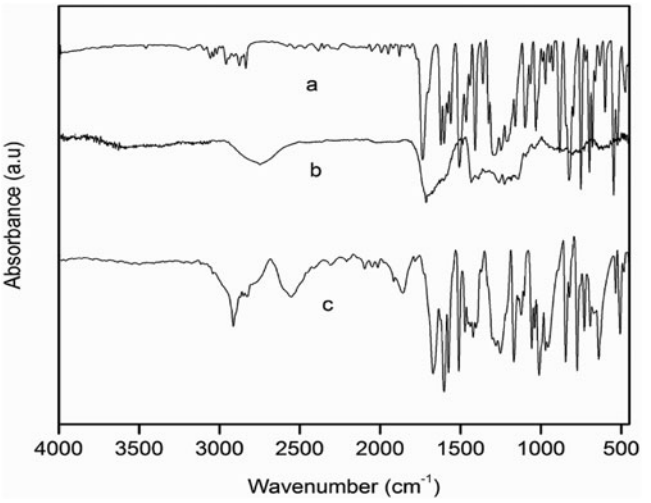

Figure 1. IR spectra of polymer and its complex: (a) pyridyl H-acceptor (N_1); (b) polymer PAA; and (c) polymer complex PAA-N_1.

be dynamic to enhance the thermotropic liquid-crystalline state [10,11]. Moreover, these liquid-crystalline networks consisting of multifunctional hydrogen bonding components, show reversible mesomorphic-isotropic phase transitions as a results of the thermal formation and breaking (ON/OFF switching) of the hydrogen bonds [12–16]. Such reversible cross-linking materials can be used to prepare dynamic materials [17–21]. Kato and Frechet first exploited two different and independent components to generate liquid crystals through intermolecular hydrogen bonding interaction, and this concept inturn resulted in numerous finding of such supramolecular liquid crystals [22]. Cui et al. reported the new series of azo pyridine supramolecular SCLCPs by H-bonding interaction. In addition the photoinduced birefringence of complexes also investigated by the complexation of various carboxylic acid derivatives [23]. Malik et al. reported the traditional important non-covalently bound liquid-crystalline polymers using a flexible carbon atom spacer and rigid aromatic core compounds [24]. Han et al. reported a supramolecular host-guest polymers for successfully used to prepare new variation of liquid-crystalline materials by poly(4-vinylpyridine) and hydroxyl cyanobiphenyl derivatives [25]. However, these reported side-chain supramolecular liquid crystals always consist of two complementary bifunctional monomers, a proton donor and a proton acceptor, which hold together through the intermolecular hydrogen bonds. To the best of our knowledge, limited studies are reported on side-chain liquid crystals generated by poly(acrylic acid) (PAA) and Schiff base derivatives through intermolecular hydrogen bonding interaction.

The aim of present study is to attach pyridyl Schiff base mesogenic derivatives to a PAA backbone through H-bonding interaction. Fig. 1 shows the structures used to construct new SCLCPs through self-assembly involving intermolecular hydrogen bonding interaction. The SCLCP complexes were characterized by using differential scanning calorimetry (DSC), polarizing optical microscopy (POM), and X-ray diffraction (XRD) analysis to determine the liquid-crystalline and thermal properties of the supramolecular complexes on dependent on the substituted spacer length.

2. Experimental Section

2.1 Materials

Tetrahydrofuran (THF) was distilled under normal pressure from sodium benzophenone ketyl under nitrogen immediately prior to use. Dichloromethane (DCM) was distilled in normal pressure over calcium hydride under nitrogen before use. Triethylaminne was distilled and dried over potassium hydroxide. *N,N'*-dicyclohexylcarbodiimide (DCC), 4-dimethylaminopryidine (DMAP), isonicotinic acid, 4-formylphenol, 4-methoxyaniline, 4-butoxyaniline, acrylic acid, and potassium carbonate were purchased from Aldrich and used as received. Other solvents were used as purified according to the standard procedure. PAA was prepared by reported literature (number average molecular weight (M_n) = 44391, weight average molecular weight (M_w) = 58263, polydispersity index (PDI) = 1.31, degree of polymer (DP) = 616, [η] = 0.21 in DMF at 30°C) [26].

2.2 Preparation of 4-formylphenylisonicotinate

To a mixture of isonicotinic acid (10 g, 0.08 mol), 4-formylphenol (9.7 g, 0.08 mol), DCC (17.8 g, 0.085 mol), and DMAP (5% w/w) were dissolved in DCM (200 mL), and the resulting mixture was stirred for 12 hr at room temperature under nitrogen atmosphere. Precipitated byproduct urea was filtered from the reaction mixture and the filtrate was concentrated by vacuum distillation. The crude product was recrystallized from *n*-hexane to get a pure white solid product. Yield 86%, ^{1}H-NMR (400 MHz, $CDCl_3$) δ (ppm): 9.91 (s, 1H, –CHO), 8.89–8.88 (m, 2H, Ar–H), 7.96–7.92 (m, 4H, Ar–H), 7.33 (d, J = 8.4 Hz, 2H, Ar–H). ^{13}C-NMR (400 MHz, $CDCl_3$) δ (ppm): 165.6 (–C=O), 157.2, 149.3, 144.7, 137.8, 123.6, 122.6, 114.7 (aromatic), and 55.8 ($–OCH_3$).

2.3 Preparation of 4-((4'-methoxyphenylimino)methyl)phenylisonicotinate (N_1)

To a mixture of 4-formylphenylisonicotinate (0.07 mol) and 4-methoxy aniline (0.07 mol), were dissolved in absolute ethanol, refluxed at 75°C for 2 hr and the resulting solution was poured to crushed ice to precipitate the product. The precipitated crude product was purified by recrystallization from ethanol to get a pure pale greenish yellow solid. Yield 91%, ^{1}H- NMR (400 MHz, $CDCl_3$) δ (ppm): 8.87–8.86 (m, 2H, Ar–H), 8.48 (s, 1H, CH=N), 8.01–7.96 (m, 4H, Ar–H), 7.33 (d, J = 8.4 Hz, 2H, Ar–H), 7.24 (d, J = 8.8 Hz, 2H, Ar–H), 6.93 (d, J = 8.8 Hz, 2H, Ar–H), 3.82 (s, 3H, $–OCH_3$). ^{13}C-NMR (400 MHz, $CDCl_3$) δ (ppm): 163.6 (–C=O), 158.6 (–CH=N), 156.8, 152.5, 150.9, 144.7, 136.7, 134.8, 129.9, 123.3, 122.3, 121.9, 114.5 (aromatic), and 55.6 ($–OCH_3$). EA: Calcd for $C_{20}H_{16}N_2O_3$: C, 72.28, H, 4.51, N, 8.43. Found: C, 72.42, H, 4.85, N, 8.42.

2.4 Preparation of 4-((4'-butoxyphenylimino)methyl)phenylisonicotinate (N_2)

4-Hydroxyacetanilide reacts with 1-bromobutane and hydrochloric acid to get 4-butoxyaniline. The desired Schiff base was prepared as for N_1. Yield 92%, ^{1}H-NMR (400 MHz, $CDCl_3$) δ (ppm): 8.66–8.85 (m, 2H, Ar–H), 8.48 (s, 1H, CH=N), 8.03–7.96 (m, 4H, Ar–H), 7.32 (d, J = 8.4 Hz, 2H, Ar–H), 7.24 (d, J = 8.8 Hz, 2H, Ar–H), 6.93 (d, J = 8.8 Hz, 2H, Ar–H), 4.02 (t, 2H, $–OCH_2–$), 1.75 (m, 2H, $–OCH_2CH_2–$), 1.48 (m, 2H, $–OCH_2CH_2CH_2–$), 1.01 (m, 3H, $–OCH_2CH_2CH_2CH_3$). ^{13}C-NMR (400 MHz, $CDCl_3$) δ (ppm): 164.3 (–C=O), 158.4 (–CH=N), 156.2, 153.2, 150.8, 144.9, 135.6,

134.8, 130.6, 123.7, 122.9, 121.8, 114.2 (aromatic), 65.4 (–OCH_2–), 32.1 (–OCH_2CH_2–), 20.6 (–OCH_2CH_2–CH_2–), and 14.5 (–$OCH_2CH_2CH_2CH_3$). EA: Calcd for $C_{23}H_{22}N_2O_3$: C, 73.79, H, 5.88, N, 7.48. Found: C, 7384, H, 5.86, N, 7.52.

2.5 Preparation of Hydrogen-Bonded Complexes

All the hydrogen-bonded side-chain polymer complexes in the present study were prepared by slow evaporation method. The polymer complexes were constructed by mixing appropriate molar ratio of H-donor polymer and pyridyl H-acceptor in the solutions of chloroform/THF (1:1 vol), which were self-assembled into supramolecules by evaporating solvents slowly. Polymeric binary complexes were prepared by mixing equimolar amounts of the PAA H-donor and two different pyridyl H-acceptor Schiff base (N_1 and N_2) molecules followed by slow evaporation method.

2.6 Measurements

Infrared spectra were recorded on a Shimadzu FT-IR 8300/8700 spectrometer in the frequency range 4000–400 cm^{-1}. The measurements were made using transparent KBr pellets, containing fine powder sample at room temperature. ^{1}H-NMR and ^{13}C-NMR spectra were measured using Joel EX-400 FT-NMR spectrometer in $CDCl_3$ with TMS as an internal standard. Gel permeation chromatography analysis were conducted on a LC-20AD/RID-10A instrument, using polystyrene as standard and THF as eluent. The intrinsic viscosity of the polymer was measured on DMF solution with an Ubbelohde viscometer at 30°C. Transition temperature and phase transition enthalpies were determined by DSC using Perkin-Elmer DSC7 calorimeter at a heating rate of 5°C per minute under nitrogen atmosphere. The liquid-crystalline texture was obtained by using Euromex polarizing microscope equipped with Linkem HFS91 heating stage and TP93 temperature programmer. Samples were made by placing between two thin glass cover slips with a heating-cooling rate of 5°C/min. Themogravimetric analysis was carried on SDT Q600 V20.5 Build 15 Universal V4.5 A TA Instruments at heating rate of 5°C/min in nitrogen. X-ray powder diffraction data for powder samples were collected on an 800 W Philips (PANANALYTICAL, Netherland) powder diffractometer using an etched glass plate sample holder by rotating anode diffractometer using Cu-Kα irradiation. Samples placed on a mettle FP 52 hot stage.

3. Results and Discussion

The PAA and pyridyl Schiff base derivatives were used as hydrogen bonding donor and acceptor. The structure of the SCLCP complexes formed by intermolecular hydrogen bonding between PAA and pyridyl Schiff base derivatives is depicted in Scheme 1. The structure of pyridyl Schiff base derivatives, such as 4-((4′-methoxyphenylimino)methyl)phenylisonicotinate (N_1) and 4-((4′-butoxy- phenylimino)methyl)phenylisonicotinate (N_2) were investigated by ^{1}H-NMR and ^{13}C-NMR measurements. NMR patterns of 4-((4′-methoxyphenylimino)methyl)phenylisonicotinate (N_1) as show the resonance peaks in the chemical shift range of 8.7–6.93 ppm attributed to the signal of aromatic proton. Meanwhile, the resonance signal of imine proton observed at 8.48 ppm (see Supporting Information). The carbonyl peak of ester group observed at 163.6 ppm, C═N signal of imine carbon at 158.6 ppm and the signal of aromatic carbon observed in the range of 156.8–114.2 ppm.

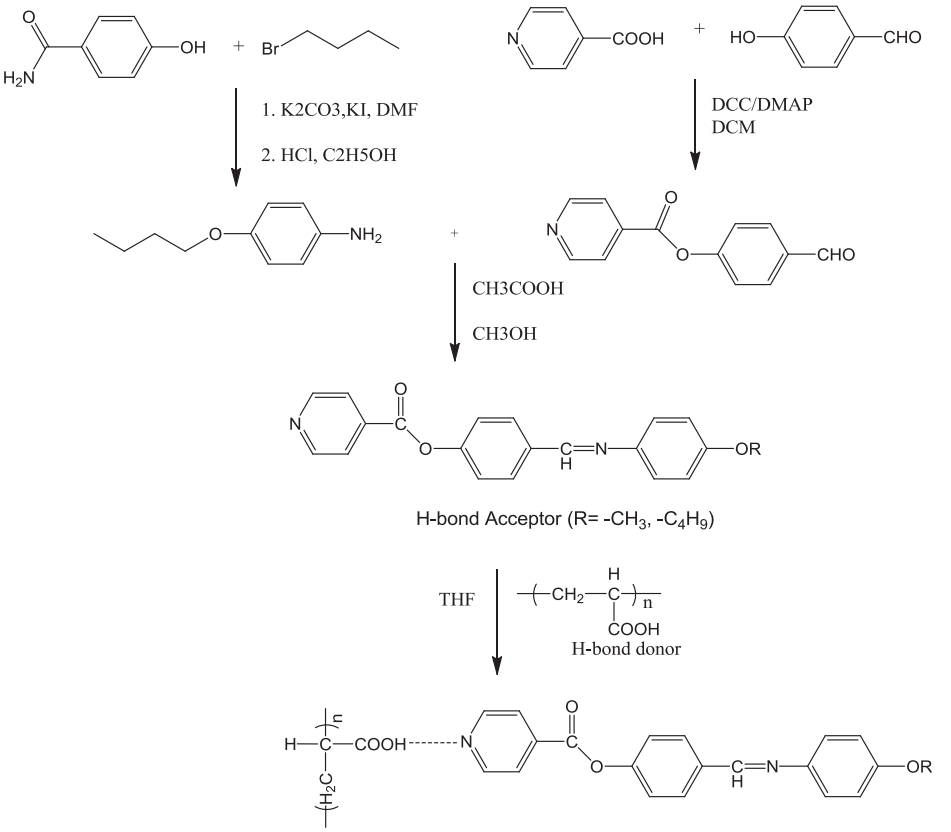

Scheme 1. Synthesis of hydrogen bonded polymer liquid crystal complexes.

3.1 IR Characterization

The existence and stability of H-bonds in polymer complexes were characterized by FT-IR spectra, and the IR spectra of hydrogen donor polymer PAA and pyridyl hydrogen acceptor N_1 were compared with that of polymer complex PAA-N_1 to examine the existence of hydrogen bonds as shown in Fig. 1. In contrast to the O−H stretching band of pure PAA at 2648 cm^{-1}, the weaker O−H stretching band observed at 2516 cm^{-1} in the complex PAA-N_1. This shifting indicates the presence of hydrogen bonding between the pyridyl group of N and acidic group of H. On the other hand, a C=O stretching vibration appeared at 1748 cm^{-1} in complex PAA-N_1, which showed that the carbonyl group is in a less associated state than in pure PAA with weaker C=O stretching vibration appeared at 1682 cm^{-1} [27,28]. The results suggested that H-bonds of polymer complex PAA–N_1 are formed between polymer PAA and H-acceptor N_1. In addition, the other polymer complexes were also confirmed to exhibit of H-bonded frameworks as polymer complex PAA-N_1, so the supramolecular structures were established in all the polymer complexes.

3.2 Formation of Liquid Crystal

In order to understand the influence of the mesomorphic behavior of side-chain polymer complexes were investigated by POM, DSC, and XRD measurements. The phase behavior

Table 1. Thermal transition parameters of H-bonded side-chain LC polymeric complexes

H-bonded complex phase transition °C (corresponding enthalpy change, J/g)				
	Heating			
PAA–N_1 (7.46)	G 53.4	SmC	178.4	I
PAA–N_2 (6.97)	G 59.6	SmC	181.2	I
PAA–(N_1–N_2) (12.7)	G 63.8	SmC	192	I

G = Glassy; SmC = smectic C; I = isotropic state.

temperature and associated enthalpy change (ΔH) of polymeric complexes are listed in Table 1. These complexes exhibited stable mesomorphic behavior. Fig. 2 shows the DSC curves of PAA-N_1 and PAA-N_2 homo polymeric and PAA(N_1/N_2) copolymeric complexes. In PAA-N_1 complex shows two endothermic peaks at 53.3 and 178.4°C. The first transition peak corresponds to glass transition (T_g) and the second peak corresponds to transition from liquid-crystalline phase to isotropic transition (T_i). The DSC curves for a PAA-N_2 complex also shows melting peak at 59.6°C, which was 6°C higher than for PAA-N_1 complex and a second endothermic peak appeared at 181.8°C, correspond to the liquid-crystalline phase to isotropic phase transition (T_i). Comparing the phase transition temperatures of PAA-N_1 complex, slight increase of isotropization temperature was observed for PAA-N_2 complex.

The existence of the mesophase was further tested explicitly using POM (shown in Fig. 3). Observations show that the polymeric complexes form liquid-crystalline properties in the temperature range between the glass transition temperature (T_g) and the isotropization temperature (T_i). In order to obtain a clear characteristic optical texture for phase identification, the complex was cooled slowly from its isotropization temperature at 2°C/min prior to

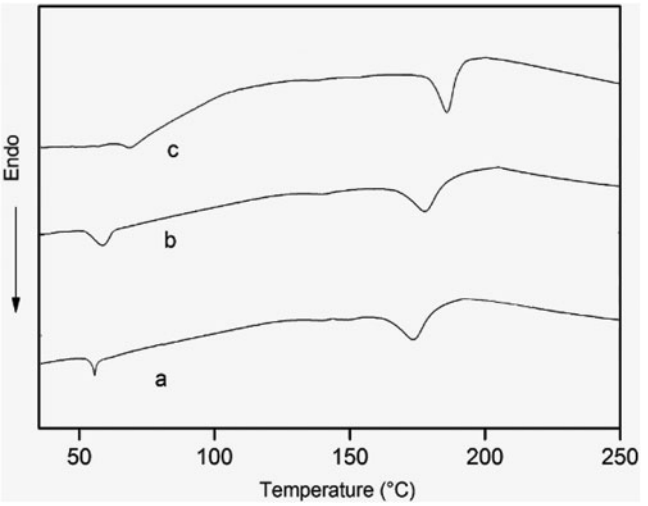

Figure 2. DSC thermograms of hydrogen bonded liquid-crystalline polymers: (a) homopolymeric complex of PAA-N_1; (b) homopolymeric complex of PAA-N_2; and (c) copolymeric complex of PAA and the 1:1 mixture of N_1 and N_2.

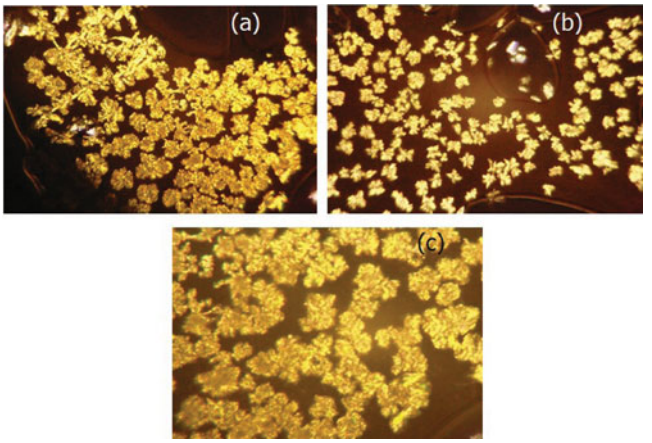

Figure 3. POM textures at the cooling process: (a) smectic C, broken fan shaped texture of PAA-N_1; (b) smectic C, broken-fan shaped texture of PAA-N_2; and (c) smectic C, broken-fan shaped texture of copolymeric complex of 1:1 mixture of N_1 and N_2.

observation of LC phase. The intermolecular H-bonded PAA-$\mathbf{N_1}$ complex formed smectic C phase broken fan shaped texture at 170°C on cooling from the isotropic phase and PAA-N_2 complex also formed smectic C phase broken fan shaped texture at 179°C, which is higher temperature than PAA-$\mathbf{N_1}$ complex. The interaction between the noncovalently assembled mesogenic units was apparently strong to drive the microphase separation needed for a smectic phase. From DSC and POM studies, both polymeric complexes exhibited smectic phase during cooling from isotropic melt.

The temperature dependent XRD patterns obtained from powder sample of PAA-$\mathbf{N_1}$ and PAA-N_2 complexes for each phase obtained on heating at 120°C are presented

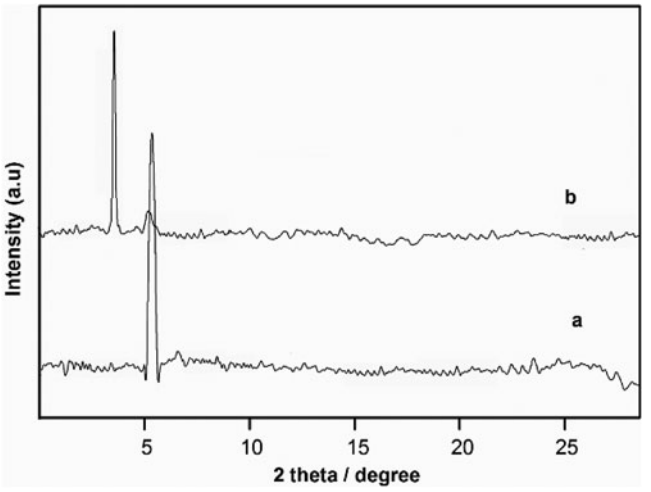

Figure 4. Powder X-ray diffraction of hydrogen bonded polymer: (a) PAA-N_1 complex at 175°C and (b) PAA-N_2 complex at 185°C.

Table 2. Thermal stability of polymer and its H-bonded LC complexes

Sample	$T_{5\%}$ (°C)	T_{max}(°C)	$T_{95\%}$(°C)
PAA	185.5	205.0	280.4
PAA-N_1	278.1	302.3	348.5
PAA-N_2	305.0	316.5	408.2

$T_{5\%}$ = 5% weight loss; T_{max} = maximum weight loss; $T_{95\%}$ = 95% weight loss.

in Fig. 4. A reflection peak at lower angles (associated with the smectic layer) is observed for PAA-N_1 and PAA-N_2 complexes. In PAA-N_1 complex show sharp reflection at $2\theta = 5.5^\circ$ corresponding d-spacing value of 16.1 Å in small angle region. The intensity curve of PAA-N_2 complex at 120°C also disclose very similar pattern (d-spacing 23.8 Å), indicating the presence of ordered smectic layer arrangements. These results indicate that the overlapping of the H-bonded mesogenic cores in the smectic layer for the complexes and inhibition of the molecular orientation fluctuations and an increase in the order of molecular arrangement.

3.3 Thermal Properties

The obtained powder complexes were subjected to thermal analysis to determine their stability behavior by thermogravimetic analysis under nitrogen atmosphere at a heating rate of 5°C/min. TGA curves showed (Fig. 5) that both the complexes are thermally more stable than the polymer. As shown in Table 2, the 5% weight loss temperature (denoted as $T_{5\%}$) of polymer and its complexes observed in the range of 185–305°C, due to the breakage of carbon atom of alkyl chain of polymer and its complexes. However, complexes exhibit a much higher temperature than polymer, which means that the thermal stability of complexes has been improved greatly due to the presence of H-bond and more cross-linking ability than polymer. This result also showed that the thermal stability increase slightly with increasing of their substituted spacer length.

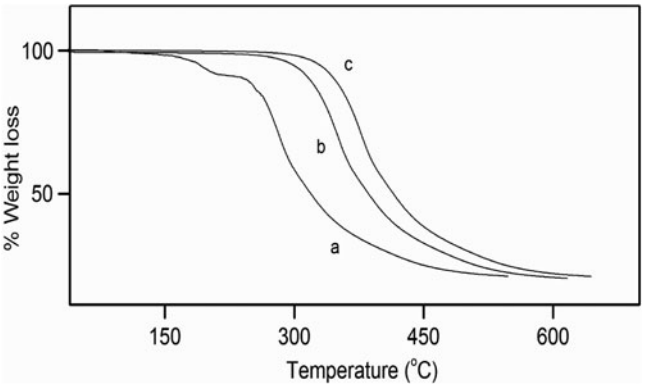

Figure 5. TGA thermograms: (a) PAA; (b) PAA-N_1; and (c) PAA-N_2.

Table 3. Smectic-isotropic change of PAA-N_1 complexes of different molar ratio

Mole fraction of N_1/mol%	ΔH/(kJ mol^{-1})
0	0.95
20	2.65
40	3.84
60	3.98
80	4.25
100	4.68

3.4 Effect of Complex Composition

Figure 6 shows the DSC curves for the first heating scans of PAA-N_1 complexes with different composition. The corresponding transition temperature and enthalpy changes are listed in Table 3. The complexes appear miscible over the entire composition range when viewed under a microscope. As can be seen in Fig. 6, when the molar ratio of N_1 to the acidic group of the PAA in the complex increased from 0.4 to 1.0 and the $T_g - T_I$ temperature range also changed. Therefore, the thermal stability of the mesogenic phase increased with increasing N_1 content in the complexes. The formation of these supramolecular SCLCP ascended from the assembly of low molar mass compounds with the polymer backbone through hydrogen-bond interactions between the acidic group of the PAA and the nitrogen group of N_1. The connection of the mesogenic unit to the polymer backbone increased the softness of the polymer backbone, which in turn hindered the movement of the mesogenic units and thus facilitated the ordered packing of the mesogenic units along a specific direction. When higher the molar ratio of N_1, forms more hydrogen-bonding mesogenic units there were in the complex and the higher the isotropization temperature was observed. The decrease in stiffness of the polymer backbone was shown by a change of T_g from 103°C. This indicated that the physico-chemical nature of the main chain affected the mesogenic behavior. As a result, the formation of SCLCP at molar ratio of 0.4 levels indicated that

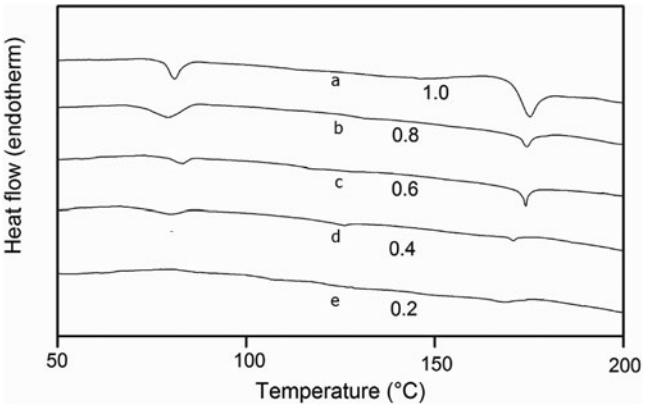

Figure 6. DSC curves of PAA-N1 complexes of different molar ratio, first heating scan: (a) 1:1, (b) 1:0.8, (c) 1:0.6, (d) 1:0.4, and (e) 1:0.2.

hydrogen-bonded PAA-N_1 complex was sufficient for the formation of a LC phase. When the molar ratio of N_1 to the polymer chain was above 1.0 molar ratio, there were insufficient acidic groups to ensure a 1:1 interaction. Some of the N_1 could not be connected to the main chain through hydrogen-bonding, although the excess N_1 could be incorporated into a liquid crystal and disrupted the ordering of the LC phase and also phase separation was not observed optically for all complexes. A similar result was observed for PAA-N_2 complex.

3.5 Formation of Supramolecular Copolymeric Complexes

The advantages of hydrogen-bonded liquid-crystalline polymers are the ease with which various copolymers can be prepared. Copolymers of any desired composition can be prepared by self-assembly of H-donor polymer and mixture of two different H-bond acceptors can control the mesomorphic properties of a copolymers. This is in contrast to conventional method in which separate monomers must be prepared.

Figure 3c shows an polarized optical micrograph of supramolecular copolymeric complex PAA-(N_1/N_2) derived from PAA and a mixture of N_1 and N_2, in which the complexes were formed using 1:1 molar ratio of hydrogen bond donor and acceptor groups. Figure 2c shows the phase transition diagram of liquid-crystalline copolymeric PAA-(N_1/N_2) complexes. Higher T_g and T_i values are observed for the copolymeric complexes than for the corresponding homopolymeric complexes due to the additional electron donor-acceptor interaction between polymeric side-chain and mesogens [25]. Furthermore, the enthalpy changes of isotropization are also significant positive deviation than those homopolymeric systems. POM studies showed that the copolymeric complexes formed a smectic C phase broken-fan shaped texture at 189°C.

4. Conclusions

The supramolecular SCLCP complexes were prepared by polymer (PAA) and pyridyl Schiff base derivatives (N_1 and N_2) through intermolecular hydrogen bonding interaction. The appropriate molar ratios of proton donor polymer and pyridyl Schiff base proton acceptor derivatives were complexed. This co-operation of noncovalent hydrogen bonding interaction resulted in the formation of liquid-crystalline polymer. The effect of substituted spacer length on liquid-crystalline properties was discussed. The supramolecular copolymeric complexes containing a 1:1 molar ratio of hydrogen bond donor polymer and a mixture of hydrogen bond acceptors were also discussed. The electron donor-acceptor interaction of copolymeric system enhanced the thermal stability of the liquid-crystalline phase. The phase behavior of complexes were investigated by DSC, POM, and XRD measurements and the results proved the presence of smectic C phase broken-fan shaped textures. This study showed that the adjusting the combination of molar ratio of different pyridyl Schiff base derivatives in copolymeric complexes could be controlled the formation of liquid-crystalline phase.

Funding

The authors acknowledge the financial support from Council of Scientific and Industrial Research (CSIR F. No. 01(2310)/09/EMR II), New Delhi, India.

References

[1] Whitesides, G. M., & Grzybowski, B. (2002). *Science*, *295*, 2418.
[2] Pollino, J. M., & Weck, M. (2005). *Chem. Soc. Rev.*, *34*, 193.
[3] Lin, H. C., Lin, Y., Lin, Y. S., Chen, Y. T., Chao, I., & Wei Li, T. (1998). *Macromolecules*, *31*, 7298.
[4] Sakthivel, P., & Kannan, P. (2004). *J. Polym. Sci. Part A: Polym. Chem.*, *42*, 5215.
[5] Price, D. J., Willis, K., Richardson, T., Ungarb, G., & Bruce, D. W. (1997). *J. Mater. Chem.*, *7*, 883.
[6] Grunert, M., Alan Howie, R., Kaedingb, A., & Imrie, C. T. (1997). *J. Mater. Chem.*, *7*, 211.
[7] Kato, T., Hirota, N., Fujishima, A., & Frechet, J. M. J. (1996). *J. Polym. Sci. Part A Polym. Chem.*, *3*, 57.
[8] Guan, L., & Zhao, Y. (2001). *J. Mater. Chem.*, *11*, 1339.
[9] Muthukumar, M., Ober, C. K., & Thomas, E. L. (1997). *Science*, *277*, 1225.
[10] Kato, T., Mizoshita, N., & Kishimoto, K. (2006). *Angew. Chem. Int. Ed.*, *45*, 38.
[11] Vasilets, N., Shandryuk, G. A., Savenkov, G. N., Shatalova, A. M., Bondarenko, G. N., Talroze, R. V., et al. (2004). *Macromolecules*, *37*, 3685.
[12] Yu, T., Zhou, Y., Zhao, Y., Liu, K., Wang, E. C. D., & Wang, F. (2008). *Macromolecules*, *41*, 3175.
[13] Xiao, S., Lu, X., Lu, Q., & Su, B. (2008). *Macromolecules*, *41*, 3884.
[14] Thibault, R. J., Hotchkiss, P. J., Gray, M., & Rotello, V. M. *J.*(2003). Am. Chem. Soc., *125*, 11249.
[15] Kato, T., Ihata, O., Ujiie, S., Tokita, M., & Watanabe, J. (1998). *Macromolecules*, *31*, 3551.
[16] Kato, T., Yasuda, T., Kamikawa, Y., & Yoshio, M. (2009). *Chem. Commun.*, 729.
[17] Kato, T., Miizoshita, N., & Kanie, K. (2001). *Macromol. Rapid. Commun.*, *22*, 797.
[18] Kanie, K., Nishii, M., Yasuda, T., Taki, T., Ujiie, S., & Kato, T. (2001). *J. Mater. Chem.*, *11*, 2875.
[19] Kanie, K., Yasuda, T., Ujiie, S., & Kato, T. (2001). *Chem. Commun.*, 1899.
[20] Kannan, P., Raja, S., & Sakthivel, P. (2004). *Polymer*, *45*, 7895.
[21] Kanie, K., Yasuda, T., Nishii, M., Ujiie, S., & Kato, T. (2001). *Chem. Lett.*, 480.
[22] Kato, T., & Frechet, J. M. J. (1989). *Macromolecules*, *22*, 3818.
[23] Cui, L., & Zhao, Y. (2004). *Chem. Mater.*, *16*, 2076.
[24] Malik, S., Dhal, K. P. K., & Mashelkar, R. A. (1995). *Macromolecules*, *28*, 2159.
[25] Han, X., Zhang, S., Shanks, R. A., & Pavel, D. (2008). *Reac. Funct. Polym.*, *68*, 1097.
[26] Kato, T., Kihara, H., Ujiie, S., Uryu, T., & Frechet, J. M. J. (1996). *Macromolecules*, *29*, 8734.
[27] Gimeno, N., Ros, M. B., Serrano, J. L., & Fuente, R. M. (2004). *Angew. Chem. Int. Ed.*, *43*, 5235.
[28] Wang, L-Y., Tsai, H-Y., & Lin, H-C. (2010). *Macromolecules*, *43*, 1277.